Contents lists available at ScienceDirect

Future Foods

Functional and flavour properties of de-oiled flours and dry-enriched protein concentrates of lupin and soy

Regina G.A. Politiek [a,b], Eirini Pegiou [b,c], Lotta L. Balfoort [a], Marieke E. Bruins [b], Maarten A. I. Schutyser [a], Julia K. Keppler [a,*]

[a] *Laboratory of Food Process Engineering, Wageningen University & Research, Wageningen, the Netherlands*
[b] *Wageningen Food & Biobased Research, Wageningen University & Research, Wageningen, the Netherlands*
[c] *Laboratory of Plant Physiology, Wageningen University & Research, Wageningen, the Netherlands*

A B S T R A C T

Dry fractionation is low in energy and water use and thus a sustainable option to obtain protein-rich ingredients. Air-classification is used to remove starch from legumes, and electrostatic separation can be used to remove fibres from other starting materials like oilseeds. Flour from oil-rich crops needs to be de-oiled to facilitate dry fractionation, which involves the use of organic solvents or mechanical pressing and might affect the ingredient functionality. This research evaluated if the functionality of soy and lupin is affected by solvent de-oiling and electrostatic separation. Industrially toasted soy and lupin flour contained native protein, which was preserved upon electrostatic separation, de-oiling with hexane and de-oiling with acetone, but ethanol de-oiling resulted in protein denaturation. De-oiling with ethanol or hexane is preferred over de-oiling with acetone based on the flavour profile after de-oiling. The use of different solvents affected the solubility to a different extent and electrostatic separation resulted in a similar or higher solubility of the ingredients (22–49 %), dependent on the solvent, crop and pH condition used. Overall, electrostatic separation resulted in protein-enriched ingredients (43 %DM - 67 %DM N_{factor}=5.7) that show potential for application as stabilizers in emulsion-based systems like dressings or frozen foam-based systems like ice-cream.

1. Introduction

For many years, foods have been created by combining ingredients that are neutral in taste and constant in quality, which resulted in the development of highly refined ingredients such as protein isolates (Lie-Piang et al., 2023). Producing protein isolates from plant-based seeds is conventionally done by wet fractionation. However, wet fractionation has a significant impact on the environment in terms of water usage, energy usage and raw material losses, which amplifies the need for more sustainable ingredients (Henchion et al., 2017; Lie-Piang et al., 2023). Dry fractionation can be used as an alternative to produce functional protein-enriched ingredients for the food industry (Schutyser et al., 2015). Here, air-classification is used to remove starch from legumes, and electrostatic separation can be used to remove fibres from other starting materials like oilseeds.

Electrostatic separation is a new dry separation technique for food ingredients, which is amongst others used to enrich components such as protein and fibre from fine milled legume flours (Vitelli et al., 2020). The

separation is based on the tribo-electric charging properties of the particles, where the charge is induced by particle-particle interactions and particle-wall interactions (Landauer et al., 2019; Xing et al., 2021). Electrostatic separation has been successfully applied to oil rich seeds (i. e. lupin), de-oiled cakes (mechanically de-oiled, ~6 and 7 % oil) and de-oiled meals (solvent de-oiled ~<1 % oil), from for example soybean, rapeseed and sunflower seeds (Ancuța and Sonia, 2020; Basset et al., 2016; Kdidi et al., 2019; Laguna et al., 2018; Xing et al., 2018). Studies on the functionality of protein-enriched fractions after tribo-electrostatic separation are scarce compared to studies on air classification or sieving but show promising results. For example, the order of combined separation steps (air classification and electrostatic separation) did not significantly affect the protein solubility of CO_2 extracted rapeseed press-cake enriched ingredients (Wockenfuss et al., 2023). Furthermore, tribo-electrostatic separation of navy bean (starch-rich crop) resulted in protein-enriched fractions with excellent emulsifying and foaming properties and showed that the native protein functionality could be preserved upon electrostatic separation

---

(Tabtabaei et al., 2019).

We therefore hypothesize that electrostatically separated fractions would similarly result in higher functionality than soy and lupin flours. However, the functionality is likely further affected by the pre-treatment steps applied. To illustrate, de-oiling is often a prerequisite for electrostatic separation of oil-rich seeds, but the choice of solvents affects the separation performance and the composition of the produced ingredients (Politiek et al., 2023). Furthermore, toasting and dehulling are generally applied as a pre-treatment steps to reduce the antinutritional factors, which can also affect the protein nativity and functionality of the fractions (Bader et al., 2011; Lawal et al., 2021).

This research aimed to evaluate if the functionality of soy and lupin is affected by solvent de-oiling and electrostatic separation. This was done by systematically studying the protein nativity and flavour of the samples after pre-processing (no de-oiling and de-oiling with acetone, ethanol and hexane) and tribo-electrostatic separation (protein-enriched fractions). Based on the flavour profiles of the samples and the electrostatic separation performance (protein purity and fraction yield) four protein-enriched ingredients were selected. The solubility of the selected ingredients was evaluated at different pH (3, 6 and 7). These pH values were chosen to represent products with lower pH like dressings (pH 3) and products with more neutral pH like ice-cream (pH 6 - pH 7). Furthermore, the emulsifying properties of the selected ingredients were assessed at pH 3 (creaming index and freeze-thaw stability) and the foamability of the ingredients was assessed at pH 6. A schematic overview of the different aspects discussed in this research is presented in Fig. 1. Lastly, an outlook is provided towards potential product application of the protein-enriched ingredients produced by electrostatic separation. Here it is expected that samples with good emulsifying properties at pH 3 will be well applicable as stabilizers in dressings, whereas samples with good foamability at pH 6 can be used as stabilizers in foam-based systems with more neutral pH like ice-creams.

2. Materials and methods

2.1. Materials

Fine impact milled toasted de-hulled soy flour (average particle size $DV_{50}=56\pm2$ μm) and toasted de-hulled lupin flour ($DV_{50}=41\pm1$ μm) were kindly provided by Frank Foods (Twello, the Netherlands). The materials were kept in screw-capped polyethylene containers at 4 °C. The toasted lupin and soy flours (400–500 g) were de-oiled for 6 h with ethanol (96 v/v%, VWR International, Rosny-sous Bois, France), acetone

(Actu-all Chemicals, Oss, The Netherlands) and hexane (Actu-all Chemicals, Oss, The Netherlands) by using a custom-built Soxhlet extractor. The de-oiled flours were left in the fume hood overnight (20 °C) to evaporate the residual solvent and consecutively, powder lumps were broken up by milling approximately 150 g of material in 500 ml bowls with a Pulverisette 5 bead mill (Fritsch GmbH, Germany), operated at 400 rpm for a total of 4 min with one min on and off as described in detail in our previous study (Politiek et al., 2023). After preparation, the samples were stored at 4 °C.

2.2. Electrostatic separation to obtain protein-enriched fractions

A custom-build electrostatic separator with a venturi tube was used to prepare the protein-enriched fractions as described by Politiek et al. (2023). For each separation approximately 100 g was fed into the vertical electrostatic separator and separated into four fractions: ground electrode (GE-V), positive electrode (PE-V), ground collector (GC-V) and positive collector (PC-V). The protein enriched fraction was obtained at the ground electrode and the depleted fraction at the positive electrode (Politiek et al., 2023). This study focussed on the functionality of the protein-enriched fractions obtained at the ground electrode (referred to as enriched fraction).

2.3. Protein denaturation

Denaturation of the samples was determined by measuring a thermogram of each sample with differential scanning calorimetry (DSC) (DSC-250, TA instruments, Newcastle, USA). 20 w/w% protein dispersions of each de-oiled flour and the enriched fraction were prepared and stirred at 1400 rpm for 2 h at 22 °C in an Eppendorf thermomixer. A large volume pan was filled with 53 ± 5 mg of protein dispersion (containing ~10 mg sample) and then well sealed. An empty pan was used as a reference. The samples were heated from 20 °C to 140 °C at a heating rate of 2 °C/min and then cooled to 20 °C. A second heating cycle was used to investigate the reversibility of the transition. The peak denaturation temperature (T_d) and the enthalpy of denaturation were determined with TRIOS software (TA Instruments).

2.4. Headspace analysis of volatile compounds with SPME GC-(O)-MS

To trap and analyse the volatile compounds, solid phase microextraction gas chromatography mass spectrometry (SPME GC–MS) was used as described previously (Pegiou et al., 2021). From each sample,
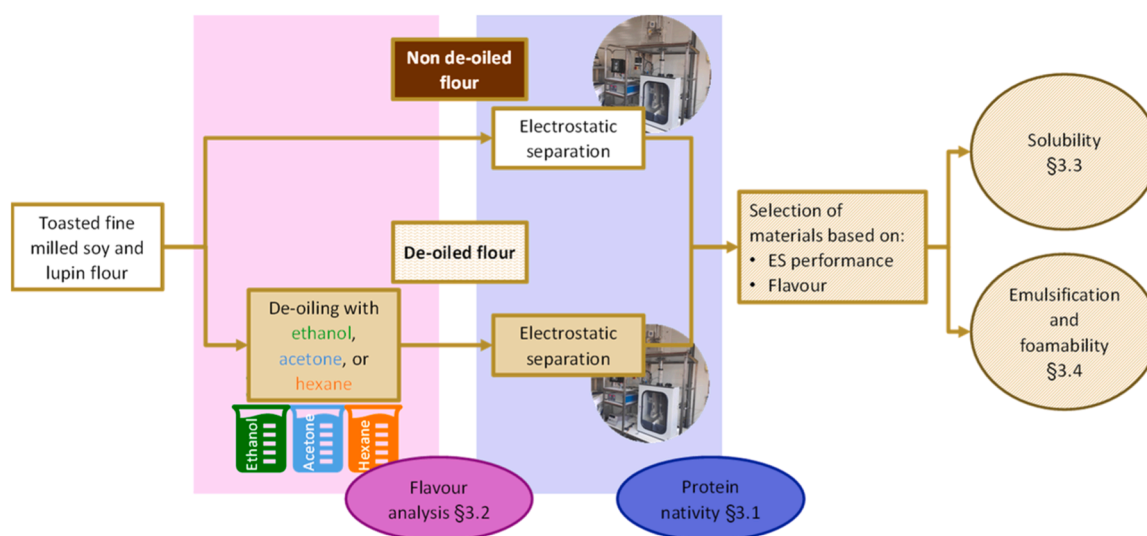
Fig. 1. Schematic overview of the overall process and functionality analysis. Electrostatic separation (ES) was done for both the non-de-oiled and the de-oiled flours. The numbers refer to the paragraphs (§) where the results are discussed.

0.5 g powder was transferred to 10-ml ND18 headspace glass vials with magnetic screw caps (8 mm opening) with silicone/PTFE septa (BGB Analtik®, Germany) and mixed with 1.5 mL NaCl-H$_2$O (26.3 w/w%) to release the volatiles to the headspace. The samples were preconditioned for 10 min at 50 °C agitating at 350 rpm. Volatiles in the headspace were afterwards trapped by inserting the SPME fibre (PDMS/DVB/CAR 50/30 μm diameter, 1 cm length, Supelco, PA, USA) to the headspace of the vial for 15 min at 50 °C without agitation (Pegiou et al., 2021). The volatiles were desorbed from the SPME fibre in split-less mode by heating the fibre at 250 °C for 2 min onto the GC column (Zebron ZB-WAX 30 m x 0.25 mm x 1.00 μm, Phenomenex, the Netherlands) via a cooled injector system (CIS4, Gerstel, Germany) with a constant helium flow of 1 ml/min (Pegiou et al., 2021). The GC oven temperature was programmed according to the settings used by Siccama et al. (2021): 2 min at 45 °C followed by a temperature increase with 8 °C/min to 200 °C, and a final rate of 15 °C/min to 250 °C, which was maintained for 3 min.

The lupin samples (none, acetone, ethanol and hexane de-oiled) were selected for evaluation with gas chromatography-olfactometry (GC—O) coupled to an MS system, to determine which peaks were odour active. For analysis with GC—O-MS double the amount of sample (1 g + 3 mL of NaCl water 26.3 w/w%) was used as the signal was split with a GC column splitter to split the signal 1:1 towards the MS and the Olfactory detection port (ODP2, Gerstel, The Netherlands). Three assessors performed sniffing and assigned the peaks of the GC—O-MS profile to specific aroma attributes and noted down the perceived aroma per compound at the given retention times, without knowing which compound corresponds to which peak as described by Pegiou et al. (2023). The sample order was randomised. Other conditions were the same as with SPME GC–MS.

2.5. Material solubility and protein solubility

Both the solubility and the protein solubility of the samples were accessed with adapted methods from Peng et al. (2021), Sweers et al. (2023) and Morr et al. (1985). For this, a 2 w/v% dispersion was prepared in a 15 mL centrifuge tube with a final volume of 10 mL. After adding 9 mL of Milli-Q water, the pH of the dispersion was determined and adjusted to pH 3, 6 and 7 until stable with 5 M HCl (Actu-All Chemicals, the Netherlands) or 5 M NaOH (Sigma-Aldrich U.S.). The volume added to adjust the pH was tracked, and the total volume of the dispersion was adjusted to reach a final volume of 10 mL. The samples were moderately shaken for 2 h at ambient temperature and subsequently centrifuged with a Sorvall Legend XFR centrifuge (Thermo Scientific™, Waltham, U.S.) at 4500 g for 20 min at 4 °C to obtain a supernatant and pellet. The pellets and supernatants were oven-dried at 105 °C and weighted (Peng et al., 2021). The initial material was also oven dried over-night to determine the dry matter content (DM) of the initial material. The overall solubility was then calculated with Eq. (1).

$$\text{Solubility}[\%] = \frac{\text{Weight supernatant}[\text{g DM}]}{\text{Weight initial material}[\text{g DM}]} 100\% \qquad (1)$$

The protein content of the oven-dried samples was determined by Dumas analysis with a rapid N exceed protein analyser (Elementar, Germany). The sample weight was 50 ± 10 mg. A protein conversion factor of N x 5.7 was used and protein contents are reported on a dry weight basis (Maclean et al., 2003). The nitrogen solubility index (NSI) was calculated with Eq. (2).

$$\text{NSI}[\%] = \frac{\text{Soluble protein}[\text{g/100g DM}]}{\text{Initial protein}[\text{g/100g DM}]} 100\% \qquad (2)$$

2.6. Emulsion preparation

Protein dispersions were prepared by mixing 1.0 w/w% protein in ~250 g phosphate buffer (10 mM, pH 3.0). A protein concentration of 1

w/w% was chosen as previous research found that this concentration could already result in narrow particle size distributions in emulsions prepared with native soybean proteins (Palazolo et al., 2011). Additionally, 1.0 w/w% salt (NaCl) was added to the dispersions to represent salt concentrations in dressings. The dispersion was gently mixed with a magnetic stirrer at 350 rpm at room temperature for 3 h (Sridharan et al., 2020). Then 30 w/w% canola oil was slowly added to the dispersions and homogenised for 1 min at 11,000 rpm with a rotor-stator homogeniser (Ultra-Turrzx IKA T18 digital, Germany). The pH was adjusted to pH 3 with 0.1 M HCl (Ray and Rousseau, 2013). The pH of the coarse emulsions was checked and adjusted if necessary. The coarse emulsions were further homogenised to reduce the droplet size and polydispersity using a colloid mill (IKA Magic Lab, Staufen, Germany) with a gap width of 0.16 mm for 2 min at a speed of 15,000 rpm. The cooling element temperature was set at 20 °C to avoid potential protein denaturation upon emulsification, this was well below the denaturation temperatures measured with DSC (Section 3.2). The emulsions were stirred with a magnetic stirrer at 250 rpm for another 30 min, and then transferred to 50 mL and 15 mL tubes. Half of the tubes were stored at 4 °C for a minimum of 3 h before further emulsion stability analysis (Sridharan et al., 2020). The other half was stored at -18 °C for at least 22 h before further freeze-thaw treatments and analysis (Zhang et al., 2017).

2.7. Emulsion stability

The emulsion stability was monitored over a period of seven days. At least four pictures were taken during the storage time, with fixed measurements on day one and day seven. The unfrozen emulsions were used as such, whereas the frozen emulsions were thawed after one day by placing them in a water bath for 2 h at 20 °C (Zhang et al., 2017). The creaming index (CI) of the emulsions and thawed emulsions was calculated with Eq. (3).

$$\text{Creaming index (CI)}[\%] = \frac{H_S}{H_T} 100\% \qquad (3)$$

Where H_S is the height of the serum layer at the bottom of the tube, H_T the total height of the emulsion (Zhang et al., 2017). H_S and H_T were measured using a ruler and Image J (version 1.52, National Institute of Health, USA). The morphology of the emulsion droplets was visualised by using light microscopy. Pictures were taken at day 1 and day 7 at 20x magnification, with a dilution of 10 times using a phosphate buffer (10 mM, pH 3.0) to visualise individual droplets.

2.8. Foamability

The foamability of the flours and protein-enriched fractions were determined by using an adapted protocol from (Yang et al., 2022). Dispersions of 1.0 w/w% protein were prepared in phosphate buffer (10 mM, pH 6.0). The dispersions were stirred on a magnetic stirrer plate for 60 min at room temperature. Afterwards, 10 mL of the solution was transferred into a cylindrical tube with a diameter of 3.33 cm. The solution was foamed for 2 min at 1000 rpm using an overhead stirrer. The cylindrical tube was transferred to a foaming set-up, where the foam height was monitored with a camera every 5 min. The samples were monitored in triplicate for a minimum of 30 min. The foam height was analysed with Image J (version 1.52, National Institute of Health, USA). The foam overrun was calculated with Eq. (4) (Yang et al., 2022).

$$\text{Foam overrun}[\%] = \frac{\text{Foam volume}[\text{mL}]}{\text{Initial liquid volume}[\text{mL}]} 100\% \qquad (4)$$

2.9. Data analysis

The statistical analysis of the data was performed by using IBM SPSS statistics version 29. Tukey post-hoc analysis was used if the variation

was homogeneous based on Levene's test for homogeneity, and Games-Howel was used when the data was not homogeneous. To test for correlation, the Pearson correlation test was performed. Here, significance was found at $p < 0.05$ (2-tailed).

3. Results and discussion

3.1. Protein nativity

The protein nativity of the flours and the protein fractions was examined with DSC (Fig. 2). The toasted lupin and soy showed a typical DSC profile with two peaks, which correspond to 7S and 11S protein (Devkota et al., 2023; Zhong and Sun, 2000). Both lupin and soy still contained native 7S protein (first peak) and 11S protein (second peak) (Fig. 2A; 2B). This transition was not reversible, as during the 2nd heating no further transitions occurred (Appendix Fig. A.1), showing that the toasted lupin and soy still contain native protein. The moisture content of lupin and soy used in this study was 11 % (Politiek et al., 2023). The retention of native protein is consistent with expectations since heating at low moisture contents usually results in limited protein denaturation, even at high temperatures (up till at least 150 °C for soy) (Geerts et al., 2018). At low moisture content, the temperature at which proteins denature increases significantly (Bühler et al., 2022). The denaturation peak temperatures and enthalpies measured with DSC vary with moisture content, but also with sample weight and scanning rate, where variation in the sample weight (2.5 mg – 10 mg) and scanning rate (0.5 °C/min to 5 °C/min) can already result in a 3 °C peak temperature difference (Morales and Kokini, 1997; Saeed et al., 2016;

Zhong and Sun, 2000). Based on that, the peak denaturation temperature values measured for soy and lupin flour are in a similar range as previously reported values (Devkota et al., 2023; Peng et al., 2021, 2023). The differences in measured peak temperatures were smaller than 3 °C for the 7S and 11S protein for lupin and soy under different conditions (Fig. 2). So de-oiling and electrostatic separation did not result in a significant change in peak temperature.

The retention of protein nativity after solvent de-oiling depended on the solvent used and the solvents showed the same effects for lupin and soy (Fig. 2A and B). De-oiling with acetone and hexane had low to no influence on the enthalpy measured, whereas the 7S protein peak disappeared upon de-oiling lupin and soy with ethanol (Fig. 2A and B). So de-oiling with ethanol resulted in complete protein denaturation of the 7S protein for both lupin and soy. The difference in retention of protein nativity can be explained by the different hydrophobicity of the solvents, where more hydrophilic solvents have a higher denaturing power towards than more hydrophobic solvents (Fukushima, 1969).

Electrostatic separation did not result in further protein denaturation for both lupin and soy, as after electrostatic separation of lupin and soy two peaks were still visible in the DSC thermograms and these had a similar peak denaturation temperature as the non-separated material (Fig. 2). The enthalpy of the 11S peak was even higher after electrostatic separation of ethanol de-oiled soy than before separation, which suggests that from the proportion of proteins present in the material relatively more native protein was collected in the enriched fraction. The preservation of native protein upon electrostatic separation is a unique property for soy protein products, as commercial produced soy flours show endothermic peaks, and thus contain native protein, but most

A

Material	Solvent	Peak 1: 7S protein		Peak 2: 11S protein	
		Enthalpy [Joule/g protein]	Peak temp T_d [°C]	Enthalpy [Joule/g protein]	Peak temp T_d [°C]
Lupin Flour	None	2.1	85.8	2.3	100.9
	Ethanol	ND	ND	2.5	99.7
	Acetone	1.9	86.1	2	101.9
	Hexane	1.7	85.8	2.1	101.4

B

Material	Solvent	Peak 1: 7S protein		Peak 2: 11S protein	
		Enthalpy [Joule/g protein]	Peak temp T_d [°C]	Enthalpy [Joule/g protein]	Peak temp T_d [°C]
Soy Flour	None	0.5	72.6	4.8	93.6
	Ethanol	ND	ND	1.9	92.6
	Acetone	0.7	72.5	5	94.3
	Hexane	0.5	73.3	4.8	94.7

C

Material	Solvent	Peak 1: 7S protein		Peak 2: 11S protein	
		Enthalpy [Joule/g protein]	Peak temp T_d [°C]	Enthalpy [Joule/g protein]	Peak temp T_d [°C]
Lupin GE fraction	None	2±0.1	85.8±0.3	2.3±0.1	101.7±1.1
	Ethanol	ND	ND	2.9±0.1	101.6±0.4
	Acetone	2.1±0.5	85.5±0.7	2.1±0.6	101.2±0.3
	Hexane	2.6±0.1	86.1±0.1	2.3±0	101.5±0.2

D

Material	Solvent	Peak 1: 7S protein		Peak 2: 11S protein	
		Enthalpy [Joule/g protein]	Peak temp T_d [°C]	Enthalpy [Joule/g protein]	Peak temp T_d [°C]
Soy GE fraction	None	0.8±0	73.2±0.3	4.9±0.3	93.7±0.2
	Ethanol	ND	ND	5.6±0.2	95.2±2.3
	Acetone	0.7±0.2	73.3±1.5	5.3±0.1	95.3±1.2
	Hexane	0.7±0.1	74.8±2.6	5.5±0.6	95.5±1.4

Fig. 2. DSC thermograms of lupin flour (A), soy flour (B), lupin GE fraction (C) and soy GE fraction (D) for non-de-oiled material, ethanol de-oiled material, acetone de-oiled material and hexane de-oiled material. The tables show the enthalpy and peak denaturation temperatures (T_d) of the samples. ND indicates that no peak was detected. The duplicate measurements for the fractions are included in Appendix Figure A.2.

commercially produced soy protein isolates and concentrates were completely denatured (no detectable peaks in the DSC thermogram), or had a lower enthalpy per g protein (3.1–3.5 Joule/g protein) (Lee et al., 2003), than the soy protein concentrates produced in this study (Fig. 2). In our previous research, we evaluated the effect of solvent (none, acetone, ethanol, and hexane) on the electrostatic separation performance of soy and lupin (Politiek et al., 2023). Electrostatic separation of toasted dehulled lupin- and soy flour resulted in protein enriched fractions with 48%DM protein and 43%DM protein respectively with a fraction yield of 27 % (Politiek et al., 2023). Polar solvents acetone and ethanol appeared favourable for dry fractionation of lupin based on composition (protein content 65–67 % DM), whereas hexane was more favourable for soy (protein content 60 % DM) in terms of protein purity and fraction yield (Politiek et al., 2023). Protein denaturation was found as an undesired side effect for ethanol de-oiling. So, next to composition the impact of solvent choice on protein nativity needs to be considered.

3.2. Acetone extraction, where does the smell come from?

The decision for one or the other pre-treatment may not only per se depend on the protein purity and fraction yield and protein nativity, but also on other properties of the ingredients. It was noticed upon performing experiments in the lab that the flavour changed after de-oiling of the flours, where some of the samples had a different or even an unpleasant off-flavour. This could be due to the formation of new volatile compounds, removal or suppression of odour active compounds or the release of volatile compounds upon de-oiling (Bader et al., 2011). The aroma of the flours de-oiled with acetone was perceived as sour and fermented, whereas the flours de-oiled with hexane had a very mild legume like aroma. The non-de-oiled material had no specific aroma and the material de-oiled with ethanol had a very mild yeast-type of aroma, which was associated with bread dough.

Aroma properties are mainly reflected by the composition of volatile organic compounds. To better understand the flavour composition of the samples and try to explain the different aromas as smelled in the lab and described above, a selection of samples was analysed with GC–MS and GC—O-MS. For GC–MS, this selection included lupin and lupin de-oiled with acetone, ethanol and hexane, and soy de-oiled with acetone and hexane. For soy, the flour de-oiled with acetone was selected to verify the results for lupin, as de-oiling with acetone resulted in unfavourable off-flavours. Soy de-oiled with hexane was selected for GC–MS because this process gave the best electrostatic separation performance for soy. As lupin and soy showed similar GC–MS spectra after de-oiling (Appendix Fig. B.1), only lupin was selected for GC—O analysis. Clear differences were observed in the volatile profiles of the various samples after de-oiling (Appendix Fig. B.1). To annotate the different peaks, the mass spectra of lupin, lupin de-oiled with acetone, ethanol and hexane and soy de-oiled with acetone and hexane were compared to those present in the NIST17 Mass Spectral Library and in-house databases. Hexanal (base peak 51 at 9.31 min) was present in the de-oiled lupin and soy flours (Appendix Fig. B.1). The hexanal peak was odour active and perceived as a grassy, fresh aroma by at least two accessors upon GC—O analysis (Table 1). This is in agreement with other literature where hexanal was identified as having a green, beany, grass or fresh aroma (Kaczmarska et al., 2018; Pegiou et al., 2020; Schindler et al., 2011). A $C_6H_{12}O$ ketone (base peak 43 at 10.31 min) was present in both acetone de-oiled soy and lupin flour and this compound was annotated as 4-hydroxy-4-methyl-2-pentanone (Appendix Fig. B.1). This ketone may have been formed by aldol condensation of two acetone molecules (McGorrin, 2007), which explains why the peak was specifically observed with GC-(O)-MS after acetone extraction and not after ethanol or hexane extraction. In addition, the aroma perceived around 10.30 min was described as mouldy/spicy in the GC—O-MS analysis. Therefore, this compound is suggested to highly contribute to the strong off-flavour of the acetone extracted lupin and soy. Focusing on the retention time (RT) window between 10 and 21 min, more volatile

Table 1

Summary of GC—O-MS results of lupin de-oiled with acetone, ethanol and hexane. Compounds were annotated by comparing their mass spectra to those in the NIST17 mass spectral library and in-house databases. When the annotation is not reliable, compounds are listed as "unknown" and as "<LOD" when the signal was below the detection limit. The compounds that could have been responsible for the mild bread dough like flavour in ethanol is highlighted in green and the compounds that could have been responsible for the sour fermented smell after de-oiling with acetone are highlighted in blue.

Average retention time (RT) [min]	Aroma attribute	Annotated compound	Smelled by at least 2 after de-oiling lupin with		
7.08	alcohol, bitter, yeast	C5 alcohol or ketone		Ethanol	
7.80	buttery, yeast	pentanal		Ethanol,	Hexane
9.35	grassy, fresh	hexanal	Acetone,	Ethanol,	Hexane
10.30	mouldy, spicy	C6H12O ketone	Acetone		
12.05	fishy, acidic	C5 alcohol		Ethanol,	Hexane
12.90	citrus, tropical, fruity	C7 ketone or C8 alcohol	Acetone,	Ethanol,	Hexane
13.09	metallic, fishy	<LOD	Acetone,	Ethanol	
14.00	beany	diacetone alcohol	Acetone		
14.40	sweaty, yeast	unknown	Acetone,	Ethanol	
14.55	citrus, tropical	nonanal	Acetone,		Hexane
15.10	sour	2-octenal or nonenal	Acetone		
15.16	off-flavour, earthy	1-octen-3-ol	Acetone,	Ethanol	
15.70	beany, buttery, yeast	? (base peak 68)	Acetone,	Ethanol	
16.17	sweet, buttery	decanal	Acetone,	Ethanol	
16.90	sweet, paint	C8 or C9 alcohol	Acetone		
17.65	fruity, flowery	Isophorone	Acetone,	Ethanol,	Hexane
18.79	yeast, sweet	unknown	Acetone		
18.91	off-flavour, earthy	unknown		Ethanol	
19.75	plastic, rubbery	unknown	Acetone,		Hexane
21.49	mouldy	aromatic compound	Acetone		

compounds were detected for lupin de-oiled with acetone (Appendix Fig. B.2). Some of these compounds were also found to be odour-active when GC—O-MS was performed. For example, the peak annotated as 2-octenal/nonenal (RT 15.10 min), 1-octen-3-ol (RT 15.16 min) or the mouldy aromatic compound (RT 21.49 min). Additional to the ketone (RT 10.30 min), these components might have been responsible for the sour and strong off-flavour that was perceived in the lab when smelling the lupin de-oiled with acetone (Table 1).

Concluding, the lupin and soy flours de-oiled with acetone had a different volatile profile compared to the other flours. Moreover, the compounds detected after de-oiling with acetone were odour-active and assigned to strong off-flavours (Table 1; Appendix B). This aligns with the findings found for lentil protein isolate, where treatment with acetone resulted in the accumulation of more volatile compounds, while treatment with isopropanol and ethanol resulted in samples with lower contents of volatile compounds (Chang et al., 2019). The accumulation of volatile compounds upon de-oiling with acetone is considered to have a negative impact on the sensory profile as it results in a lower consumer acceptance (Bader et al., 2011). Consumer acceptance is mainly based on sensory properties such as texture, flavour and taste (Lesme et al., 2020). Therefore, the flours de-oiled with ethanol or hexane are expected to have a higher consumer acceptance based on their flavour profiles and these are thus considered as favourable solvents to de-oil soy and lupin flour with prior to electrostatic separation. As the polar solvents were more favourable for electrostatic separation of lupin (Politiek et al., 2023) and ethanol de-oiled lupin had a better flavour profile than acetone de-oiled lupin, ethanol was chosen to de-oil lupin and hexane was chosen to de-oil soy.

3.3. Solubility of enriched fractions

The solubility and the nitrogen solubility index of the flours and fractions were determined at pH 3, pH 6 and pH 7. This section focusses on the results of the selected samples, which are lupin, lupin de-oiled with ethanol, soy and soy de-oiled with hexane and the corresponding protein enriched fractions. The solubilities of acetone de-oiled lupin and soy, hexane de-oiled lupin and ethanol de-oiled soy are included in the solubility analysis to allow further generalization of the results.

The solubility of lupin was significantly higher at pH 3 and pH 7 than pH 6 (Fig. 3A), whereas for soy the solubility was not significantly different at pH 3, 6 and 7 (Fig. 3B). To evaluate whether the solubility of

soy could be further increased upon extremer pH, the solubility of soy was also measured at pH 8 (33 %), which was significantly higher (P-value=0.006) than the solubilities at pH 3, 6 and 7. The low solubility of both legume flours at pH 6 can be explained by typical protein solubility curves, which show a high solubility at acidic pH, low solubility (<20 %) around the isoelectric point (pH 4 – pH 6) and again a high solubility at basic pH (Ma et al., 2022; Shrestha et al., 2021). The higher solubility at extremer pH conditions is caused by the positive charge of the proteins at acidic pH and negative charge of the proteins at basic pH, which results in weak hydrogen bonds between protein and water. These protein-water interactions are essential for the protein solubility (Torres et al., 2007). To confirm that the increase in solubility was caused by an increase in protein solubility, a correlation test was executed. Here, the solubility and nitrogen solubility index were positively correlated (P-value <0.001) (Appendix Fig. C.1).

The solubility of lupin and soy was affected upon de-oiling, where the effect (increased, similar or decreased solubility) depended on the solvent used. Upon de-oiling lupin with ethanol the solubility decreased (Fig. 3A). The lower solubility after ethanol de-oiling is caused by the denaturation of native protein compared to the non-de-oiled flour as also evident by DSC (Fig. 2) and in accordance with others (Bader et al., 2011; Ma et al., 2022). De-oiling soy with ethanol also resulted in a lower solubility than the non-de-oiled flour (Fig. 3B), so the lower solubility observed after de-oiling with ethanol was independent of the legume used and caused by the decreased protein nativity. De-oiling soy with hexane increased the solubility at pH 3 and pH 7 (Fig. 3). The higher solubility after de-oiling with hexane might be attributed to the lower oil content or distinctions of protein subunits as was found by Yue et al. (2021) upon de-oiling oat with hexane. However, the higher solubility after de-oiling with hexane is legume dependent as hexane de-oiled lupin (Fig. 3), or hexane de-oiled lupin flakes (Bader et al., 2011), resulted in a similar solubility as the non-de-oiled lupin flour. Acetone de-oiling resulted in similar solubilities for lupin and similar or higher (at pH 3) solubilities for soy, which was comparable to the observations for hexane de-oiling of both legumes (Fig. 3). So, hexane and acetone de-oiling do not negatively affect the material solubility, whereas ethanol de-oiling decreases the solubility.

Electrostatic separation did not negatively affect the solubility of the protein enriched fractions (Fig. 3). The lupin protein-enriched fractions had a similar or slightly higher (not significantly) solubility, whereas the soy protein-enriched fractions had a significantly higher solubility at pH
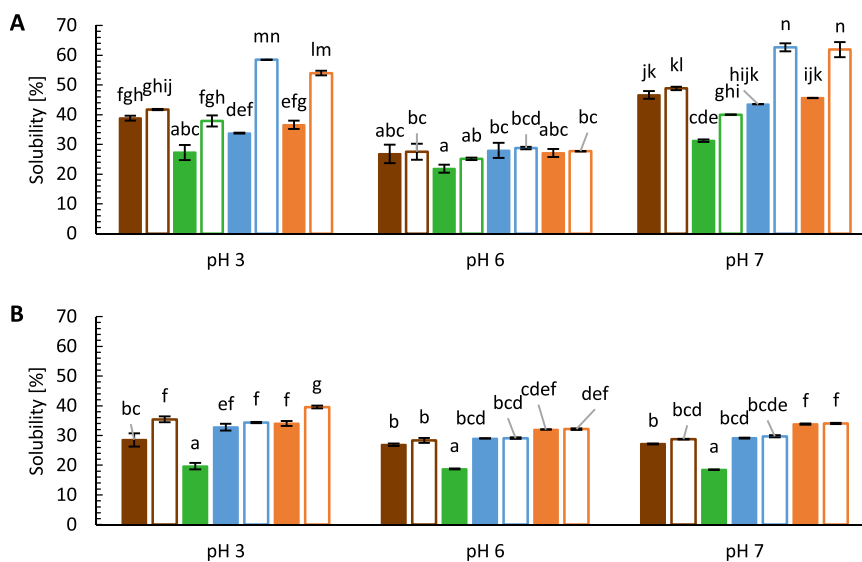
Fig. 3. Solubility of lupin samples (A) and soy samples (B) at pH 3, pH 6 and pH 7. The solid bars indicate the non-de-oiled flour (brown), ethanol de-oiled flour (green), acetone de-oiled flour (blue) and hexane de-oiled flour (orange). The white-filled bars represent the enriched fractions of the corresponding flours. The error bars represent the standard deviation and different letters indicate a significantly different solubility (*P*<0.05).

3 (Fig. 3). The solubility of ethanol, acetone and hexane de-oiled lupin increased significantly at pH 3 and pH 7 after electrostatic separation (Fig. 3A), and electrostatic separation of hexane de-oiled soy also resulted in a significantly higher solubility at pH 3 (Fig. 3B). This was caused by a higher protein solubility, so the results point towards a higher ratio of soluble proteins in the protein-enriched fractions than in the flour. The ratio of soluble proteins versus insoluble proteins might have changed after electrostatic separation because smaller particles (i. e. protein bodies) are easier caught by the electrodes than the larger poorly soluble aggregated particles, due to the higher charging capacity of small particles (Basset et al., 2016; Tang et al., 2009). The solubility of electrostatic separated hexane de-oiled soy was not significantly higher at pH 7, as was observed for hexane de-oiled lupin. This might be attributed to the generally lower solubility of soy than the solubility of lupin at pH 3 and pH 7, which is caused by a difference in nitrogen solubility curves. The nitrogen solubility curve was steeper for lupin than for soy when moving away from the isoelectric point (Appendix Fig. C.2). So, at extremer pH the solubility might also be significantly higher after electrostatic separation of hexane de-oiled soy.

The nitrogen solubility of soy flour (4–10 %) was in a similar range as reported for commercially produced soy flours and showed a similar solubility pattern as flours with a reported solubility below 20 % around pH 3 (Lee et al., 2003). The nitrogen solubilities of toasted lupin flour (64 ± 1 %) and the protein-enriched fraction from toasted lupin flour (65 ± 1 %) at pH 7 were similar to the nitrogen solubility of lupin protein isolate (64 ± 3 %) previously reported, which was de-oiled with n-hexane prior to the wet fractionation (Schlegel et al., 2019). However, the harsher conditions (i.e. longer temperature exposures or higher acidic environment) upon wet fractionation at larger commercial scale likely will result in lower solubility (Ma et al., 2022). Next to that, even without de-oiling, the lupin samples already showed high solubility at pH 3 and pH 7 (Fig. 3). So, producing protein concentrates with similar solubility as de-oiled wet fractionated lupin protein isolates via

electrostatic separation, is a huge advantage as there is less risk of a reduction in protein solubility upon industrially processing and the protein-enriched fractions might even have superior functionality over the wet fractionated material as was found for electrostatically separated navy bean (Tabtabaei et al., 2019).

3.4. Emulsification and foamability of lupin and soy enriched fractions

Emulsions with non-de-oiled lupin, ethanol de-oiled lupin, non-de-oiled soy and hexane de-oiled soy and the corresponding protein enriched fractions were prepared at pH 3 to screen whether they could be applied in dressing like emulsions (pH 3, 30 % oil) and the creaming index was monitored over time. The emulsions prepared without de-oiling lupin had a lower creaming index than the emulsions prepared with non-de-oiled soy (Fig. 4). This was likely caused by the higher solubility of lupin at pH 3 than soy at pH 3 (Fig. 3). A positive correlation between solubility and emulsifying properties has also been confirmed by many other studies (Burger and Zhang, 2019). De-oiling lupin with ethanol resulted in an increased creaming index (Fig. 4A, D, E), which might be caused by the denatured protein and less soluble material after ethanol de-oiling. For soy, de-oiling with hexane resulted in a slightly lower creaming index and also colour wise a more milk like emulsion (Fig. 4B, I and J). The lower creaming index after hexane de-oiling might also have been caused by the increased solubility after hexane de-oiling (Fig. 3B). The more milk-like colour is caused by a smaller droplet size in the emulsion with the hexane de-oiled soy than toasted soy (Appendix Fig. D.1), which leads to a stronger light scattering and therefore to a whiter, milk-like appearance of the emulsion (Fan et al., 2023).

After electrostatic separation the creaming index remained similar for the non-de-oiled lupin protein-enriched fractions, but was even worse for the protein-enriched fractions after electrostatic separation of ethanol de-oiled lupin (Fig. 4A, C, F), even though the solubility of the enriched fraction was higher (Fig. 3). The reason behind the poorer
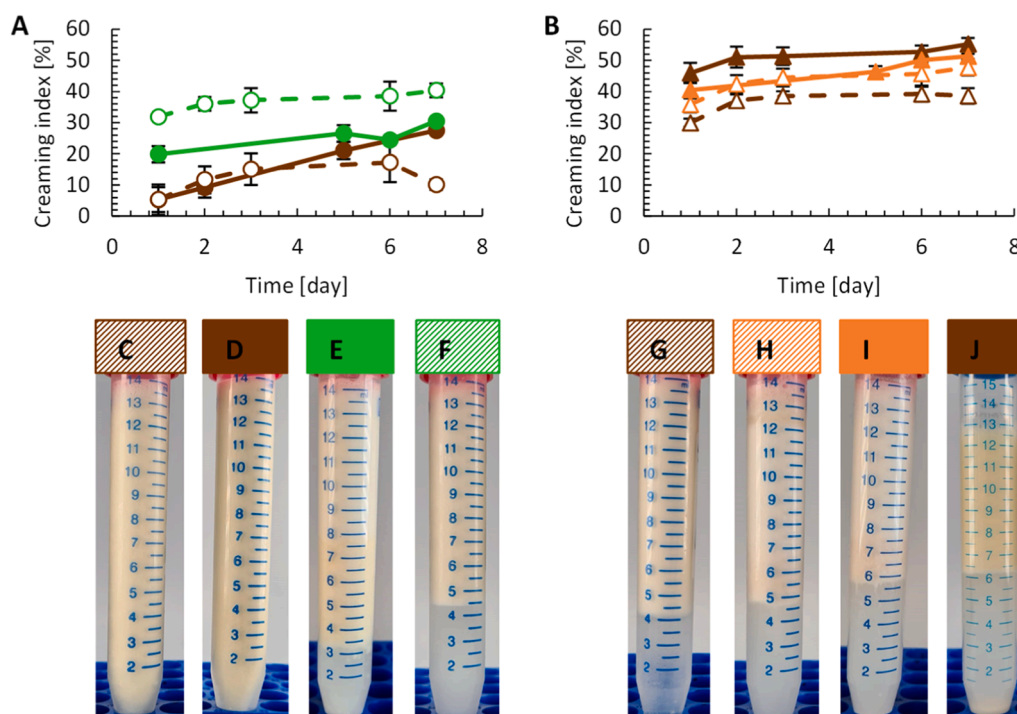
Fig. 4. Creaming index of lupin (A) and soy (B) at pH 3 (1 w/w% protein). The solid lines and symbols represent the non-de-oiled flour (brown), ethanol de-oiled flour (green) and hexane de-oiled flour (orange). The dashed lines and open symbols represent the enriched fractions of the corresponding flours. The error bars represent the standard deviation. Pictures of the emulsions after 1 day are provided from best to worst for lupin (C-F) and for soy (G-J), which were lupin enriched fraction (C), lupin flour (D), lupin ethanol (E), lupin ethanol enriched fraction (F), soy enriched fraction (G), soy hexane enriched fraction (H), soy hexane (I) and soy flour (J).
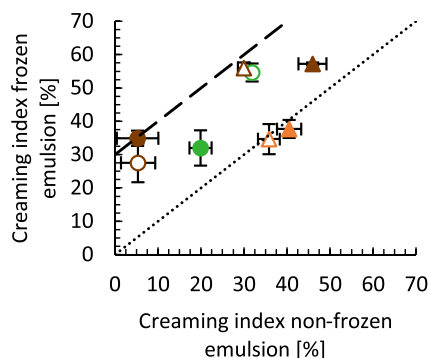
Fig. 5. Creaming index after freeze-thaw treatment against creaming index without freeze thaw treatment of lupin samples (circles) and soy samples (triangles). The solid symbols represent the non-de-oiled flour (brown), ethanol de-oiled flour (green) and hexane de-oiled flour (orange). The open symbols represent the enriched fractions of the corresponding flours. The error bars represent the standard deviation. The dotted line represents 0 % destabilisation and the dashed line represents 30 % destabilisation relative to the initial emulsion. The closer to the $y = x$ line the better the freeze-thaw stability.

emulsification might be that there is less dry matter added in the emulsion with the enriched fraction and that the other components present in the ethanol de-oiled lupin, such as carbohydrates, contributed to the emulsion stability by increasing the viscosity of the continuous phase (Funke et al., 2022; Zhou et al., 2020). For soy, the enriched fractions had a similar creaming index for soy de-oiled with hexane and for non-de-oiled soy the creaming index decreased the most after electrostatic separation and the colour of the emulsion was also more milk like after separation (Fig. 4B and G). This follows a similar pattern as was observed for the solubility of soy, which improved after de-oiling with hexane and consecutive electrostatic separation. The non-de-oiled lupin protein-enriched fraction was most promising for (non-frozen) dressing like emulsions. The other protein-enriched fractions also show potential for dressing like applications, but this would likely require a higher mass fraction to form emulsions with a lower creaming index than presented in Fig. 4.

Next to the creaming index, the freeze thaw stability was evaluated for potential frozen applications. The creaming indices measured after thawing the frozen emulsions in our study can be divided into two groups; one with a creaming index between 25 and 35 % and one with a creaming index above 50 % after thawing (Fig. 5). The hexane de-oiled soy and the corresponding enriched fraction were not destabilized after freeze-thaw treatment as the creaming indices with and without freezing were the same (Fig. 5). This is a unique property as frozen emulsions are usually significantly destabilized after thawing (Ghosh and Coupland, 2008; Zhang et al., 2017). To illustrate, an emulsion prepared with soy protein isolate at extremer pH value (pH 8) with less oil (20 %) and more protein (1.5 %) destabilised with 45 % relative to the initial emulsion (Zhang et al., 2017), while the conditions used were more favourable

(extremer pH, less oil and more protein) than the emulsification conditions used in the present study. So, the hexane de-oiled soy flour and the enriched fraction produced after electrostatic separation of hexane-de-oiled soy are most promising for frozen applications. The lupin, lupin enriched fraction and the ethanol de-oiled lupin showed a similar creaming index (25–35 %), so the samples were not completely destabilized (<30 % relative to the initial emulsion, dashed line Fig. 5) after freezing and might also be promising for frozen applications. The frozen emulsions with creaming indices above 50 % are considered to be unfavorable for frozen applications, as these were most destabilised.

To evaluate whether the flours and enriched fractions would be applicable in foam-based systems like ice-creams, they were foamed at pH 6 and the foam volume was measured over time. The foam overrun was used as a measure of the relative foam volume to the initial liquid volume (Eq. (4)). The foam abilities (foam overrun at $t = 0$) of soy and lupin were similar (27–28 %) and de-oiling resulted in a higher foam overrun for both lupin and soy (Fig. 6). This can be explained by the reduction of the oil concentration, as at high oil concentration, the oil leads to coalescence of the foam bubbles during the foam generation process by disrupting the foam films (Arnaudov et al., 2001). Next to that, the hexane de-oiled soy had a higher solubility than the soy flour and a smaller particle size (Politiek et al., 2023), which can also explain the better foamability (Moll et al., 2022). The foam overruns of the non-de-oiled lupin and soy flours were not significantly different from the foam overruns of the corresponding protein-enriched fractions, which is likely due to the low initial foamability caused by the higher initial oil content of the samples. The foam overruns of the protein enriched fractions of lupin de-oiled with ethanol and soy de-oiled with hexane were similar or slightly lower than the unseparated material, which might be because less dry matter is added to the foams prepared from the enriched fractions. As hexane de-oiling improved the foamability more than ethanol de-oiling the solvent used likely affected the foamability of the materials, next to the oil content. Overall, as hexane de-oiling combined with electrostatic separation also resulted in a good freeze-thaw stability next to the high foamability, the enriched fractions after electrostatic separation of hexane de-oiled soy have most potential for frozen applications like ice-cream.

4. Conclusion

The functionalities and flavour profile of the soy and lupin protein-enriched fractions obtained after electrostatic separation were affected by the de-oiling method. Industrially toasted and milled lupin and soy flours could be used as a starting material to produce functional protein-enriched ingredients with electrostatic separation. No de-oiling, hexane de-oiling and acetone de-oiling were favourable pre-treatments to preserve native protein, whereas ethanol and hexane de-oiling were preferred solvents over acetone for a better flavour profile of the produced ingredients. Electrostatic separation was favorable for the solubility of lupin and de-oiled lupin, where pH 7 showed the highest solubility for the lupin-based ingredients and for soy electrostatically
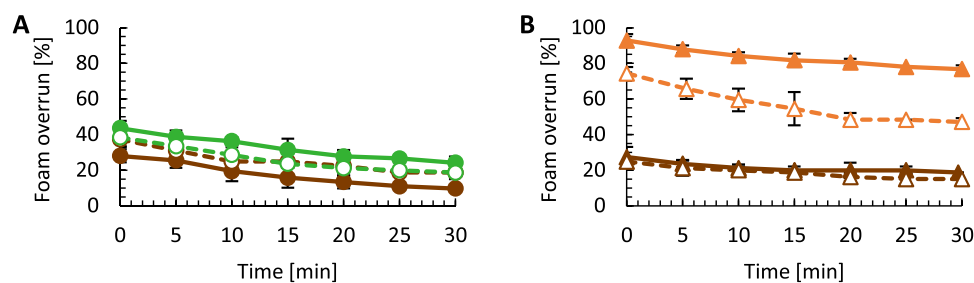
Fig. 6. Foam overrun against time for lupin (A) and soy (B) at pH 6, 1 w/w% protein. The solid lines and symbols represent the non-de-oiled flour (brown), ethanol de-oiled flour (green) and hexane de-oiled flour (orange). The dashed lines and open symbols represent the enriched fractions of the corresponding flours. The error bars represent the standard deviation, lines are added to guide the eye.

separated hexane de-oiled soy resulted in the highest solubility at pH 3. The protein-enriched fractions had equal or better functionality than the flours, except for emulsification of ethanol de-oiled lupin.

For emulsion-based applications at pH 3, no de-oiling appears necessary prior to electrostatic separation of lupin. For soy, either no de-oiling or hexane de-oiling could be used as a pre-treatment to obtain protein-enriched ingredients for emulsion-based applications like dressings, but a higher amount of the ingredient should be added to produce emulsions with more similar properties as the lupin protein-enriched ingredient. For foam-based applications de-oiling seems necessary as the presence of oil negatively affected foam stability. Overall, the results in this study can be used as a starting point to further optimize lupin and soy protein-enriched ingredients for food applications.

Funding declaration

Ethical statement

The authors declare that verbal informed consent of the participants was obtained prior to participating in aroma evaluation with GC—O-MS. They were able to withdraw from smelling the samples at any time without giving a reason. The tested products were not consumed.

CRediT authorship contribution statement

Regina G.A. Politiek: Conceptualization, Methodology, Formal analysis, Investigation, Writing – original draft. **Eirini Pegiou:** Methodology, Formal analysis, Writing – review & editing. **Lotta L. Balfoort:** Conceptualization, Methodology, Formal analysis. **Marieke E. Bruins:** Conceptualization, Supervision, Writing – review & editing, Funding acquisition. **Maarten A.I. Schutyser:** Supervision, Writing – review & editing, Funding acquisition. **Julia K. Keppler:** Supervision, Writing – review & editing, Conceptualization.

Declaration of Competing Interest

The authors declare that they have no known competing financial interests or personal relationships that could have appeared to influence the work reported in this paper.

Data availability

Data will be made available on request.

Supplementary materials

Supplementary material associated with this article can be found, in the online version, at doi:10.1016/j.fufo.2023.100274.

References

Ancuța, P., Sonia, A., 2020. Oil press-cakes and meals valorization through circular economy approaches: a review. Appl. Sci. 10 (21), 1–31. https://doi.org/10.3390/app10217432 (Switzerland).

Arnaudov, L., Denkov, N.D., Surcheva, I., Durbut, P., Broze, G., Mehreteab, A., 2001. Effect of oily additives on foamability and foam stability - 1. Role of interfacial properties. Langmuir 17 (22), 6999–7010. https://doi.org/10.1021/la010600r.

Bader, S., Oviedo, J.P., Pickardt, C., Eisner, P., 2011. Influence of different organic solvents on the functional and sensory properties of lupin (Lupinus angustifolius L.) proteins. LWT Food Sci. Technol. 44 (6), 1396–1404. https://doi.org/10.1016/j.lwt.2011.01.007.

Basset, C., Kedidi, S., Barakat, A., 2016. Chemical- and solvent-free mechanophysical fractionation of biomass induced by tribo-electrostatic charging: separation of proteins and lignin. ACS Sustain. Chem. Eng. 4 (8), 4166–4173. https://doi.org/10.1021/acssuschemeng.6b00667.

Bühler, J.M., van der Goot, A.J., Bruins, M.E., 2022. Quantifying water distribution between starch and protein in doughs and gels from mildly refined faba bean fractions. Curr. Res. Food Sci. 5, 735–742. https://doi.org/10.1016/j.crfs.2022.03.013.

Burger, T.G., Zhang, Y., 2019. Recent progress in the utilization of pea protein as an emulsifier for food applications. In: Trends in Food Science and Technology, 86. Elsevier Ltd, pp. 25–33. https://doi.org/10.1016/j.tifs.2019.02.007. Vol.

Chang, C., Stone, A.K., Green, R., Nickerson, M.T., 2019. Reduction of off-flavours and the impact on the functionalities of lentil protein isolate by acetone, ethanol, and isopropanol treatments. Food Chem. 277 (3), 84–95. https://doi.org/10.1016/j.foodchem.2018.10.022.

Devkota, L., Kyriakopoulou, K., Bergia, R., Dhital, S., 2023. Structural and thermal characterization of protein isolates from australian lupin varieties as affected by processing conditions. Foods 12 (5). https://doi.org/10.3390/foods12050908.

Fan, H., Zhu, P., Hui, G., Shen, Y., Yong, Z., Xie, Q., Wang, M., 2023. Mechanism of synergistic stabilization of emulsions by amorphous taro starch and protein and emulsion stability. Food Chem. 424 https://doi.org/10.1016/j.foodchem.2023.136342.

Fukushima, D., 1969. Denaturation of soybean proteins by organic solvents. Cereal Chem. 46 (2), 156–163.

Funke, M., Boom, R., Weiss, J., 2022. Dry fractionation of lentils by air classification - Composition, interfacial properties and behavior in concentrated O/W emulsions. LWT 154, 112718. https://doi.org/10.1016/j.lwt.2021.112718.

Geerts, M.E.J., Dekkers, B.L., van der Padt, A., van der Goot, A.J., 2018. Aqueous fractionation processes of soy protein for fibrous structure formation. Innov. Food Sci. Emerg. Technol. 45, 313–319. https://doi.org/10.1016/j.ifset.2017.12.002.

Ghosh, S., Coupland, J.N., 2008. Factors affecting the freeze-thaw stability of emulsions. Food Hydrocoll. 22 (1), 105–111. https://doi.org/10.1016/j.foodhyd.2007.04.013.

Henchion, M., Hayes, M., Mullen, A.M., Fenelon, M., Tiwari, B., 2017. Future protein supply and demand: strategies and factors influencing a sustainable equilibrium. Foods 6 (7), 1–21. https://doi.org/10.3390/foods6070053.

Kaczmarska, K.T., Chandra-Hioe, M.V., Frank, D., Arcot, J., 2018. Aroma characteristics of lupin and soybean after germination and effect of fermentation on lupin aroma. LWT 87 (1), 225–233. https://doi.org/10.1016/j.lwt.2017.08.080.

Kdidi, S., Vaca-medina, G., Peydecastaing, J., Oukarroum, A., Fayoud, N., Barakat, A., 2019. Electrostatic separation for sustainable production of rapeseed oil cake protein concentrate: effect of mechanical disruption on protein and lignocellulosic fiber separation. Powder Technol. 344 (2), 10–16. https://doi.org/10.1016/j.powtec.2018.11.107.

Laguna, O., Barakat, A., Alhamada, H., Durand, E., Baréa, B., Fine, F., Villeneuve, P., Citeau, M., Dauguet, S., Lecomte, J., 2018. Production of proteins and phenolic compounds enriched fractions from rapeseed and sunflower meals by dry fractionation processes. Ind. Crops Prod. 118 (4), 160–172. https://doi.org/10.1016/j.indcrop.2018.03.045.

Landauer, J., Aigner, F., Kuhn, M., Foerst, P., 2019. Effect of particle-wall interaction on triboelectric separation of fine particles in a turbulent flow. Adv. Powder Technol. 30 (5), 1099–1107. https://doi.org/10.1016/j.apt.2019.03.006.

Lawal, S.O., Idowu, A.O., Malomo, S.A., Badejo, A.A., Fagbemi, T.N., 2021. Effect of toasting on the chemical composition, functional and antioxidative properties of full fat and defatted sesame (sesamum indicum L) seed flours. J. Culin. Sci. Technol. 19 (1), 18–34. https://doi.org/10.1080/15428052.2019.1681333.

Lee, K.H., Ryu, H.S., Rhee, K.C., 2003. Protein solubility characteristics of commercial soy protein products. J. Am. Oil Chem. Soc. 80 (1), 85–90. https://doi.org/10.1007/s11746-003-0656-6.

Lesme, H., Rannou, C., Famelart, M.H., Bouhallab, S., Prost, C., 2020. Yogurts enriched with milk proteins: texture properties, aroma release and sensory perception. Trends Food Sci. Technol. 98 (4), 140–149. https://doi.org/10.1016/j.tifs.2020.02.006.

Lie-Piang, A., Yang, J., Schutyser, M.A.I., Nikiforidis, C.V., Boom, R.M., 2023. Mild Fractionation for More Sustainable Food Ingredients. Annu. Rev. Food Sci. Technol. 14, 473–493. https://doi.org/10.1146/annurev-food-060721, 2023.

Ma, K.K., Greis, M., Lu, J., Nolden, A.A., McClements, D.J., Kinchla, A.J., 2022. Functional Performance of Plant Proteins. Foods 11 (4), 594. https://doi.org/10.3390/foods11040594.

Maclean, W.C., Harnly, J.M., Chen, J., Chevassus-Agnes, S., Gilani, G., Livesey, G., Mathioudakis, B., Munoz De Chavez, M., Devasconcellos, M.T., & Warwick, P. (2003). Methods of food analysis. In Food Energy - Methods of analysis and conversion factors.

McGorrin, R.J., 2007. Chapter 9 Character-impact flavor compounds. R. Marsili Sensory-Directed Flavor Analysis. Taylor & Francis Group, pp. 223–267.

Moll, P., Salminen, H., Griesshaber, E., Schmitt, C., Weiss, J., 2022. Homogenization improves foaming properties of insoluble pea proteins. J. Food Sci. 87 (10), 4622–4635. https://doi.org/10.1111/1750-3841.16320.

Morales, A., Kokini, J.L., 1997. Glass transition of soy globulins using differential scanning calorimetry and mechanical spectrometry. Biotechnol. Prog. 13 (5), 624–629. https://doi.org/10.1021/bp9700519.

Morr, C.V., German, B., Kinsella, J.E., Regenstein, J.M., Buren, J.P.V., Kilara, A., Lewis, B.A., Mangino, M.E., 1985. A collaborative study to develop a standardized food protein solubility procedure. J. Food Sci. 50 (6), 1715–1718. https://doi.org/10.1111/j.1365-2621.1985.tb10572.x.

Palazolo, G.G., Sobral, P.A., Wagner, J.R., 2011. Freeze-thaw stability of oil-in-water emulsions prepared with native and thermally-denatured soybean isolates. Food Hydrocoll. 25 (3), 398–409. https://doi.org/10.1016/j.foodhyd.2010.07.008.

Pegiou, E., Mumm, R., Acharya, P., de Vos, R.C.H., Hall, R.D., 2020. Green and white asparagus (Asparagus officinalis): a source of developmental, chemical and urinary intrigue. Metabolites 10 (1), 1–23. https://doi.org/10.3390/metabo10010017.

Pegiou, E., Siccama, J.W., Mumm, R., Zhang, L., Jacobs, D.M., Lauteslager, X.Y., Knoop, M.T., Schutyser, M.A.I., Hall, R.D., 2023. Metabolomics and sensory evaluation of white asparagus ingredients in instant soups unveil important (off-) flavours. Food Chem. 406 (4), 134986 https://doi.org/10.1016/j.foodchem.2022.134986.

Pegiou, E., Zhu, Q., Pegios, P., De Vos, R.C.H., Mumm, R., Hall, R.D., 2021. Metabolomics reveals heterogeneity in the chemical composition of green and white spears of asparagus (A. officinalis). Metabolites 11 (10), 1–19. https://doi.org/10.3390/metabo11100708.

Peng, Y., Kyriakopoulou, K., Ndiaye, M., Bianeis, M., Keppler, J.K., & van der Goot, A.J. (2021). Characteristics of soy protein prepared using an aqueous ethanol washing process. Foods, 10(9), 2222. 10.3390/foods10092222.

Peng, Y., Zhao, D., Li, M., Wen, X., Ni, Y., 2023. Production and functional characteristics of low-sodium high-potassium soy protein for the development of healthy soy-based foods. Int. J. Biol. Macromol. 226, 1332–1340. https://doi.org/10.1016/j.ijbiomac.2022.11.244.

Politiek, R.G.A., Dijkink, B.H., Boogaard, L.V.D., Keppler, J.K., Schutyser, M.A.I., Bruins, M.E, 2023. Comparing electrostatic separation of soy and lupin: effect of de-oiling by solvent extraction. LWT Food Sci. Technol. 187 (9), 115290 https://doi.org/10.1016/j.lwt.2023.115290.

Ray, M., Rousseau, D., 2013. Stabilization of oil-in-water emulsions using mixtures of denatured soy whey proteins and soluble soybean polysaccharides. Food Res. Int. 52 (1), 298–307. https://doi.org/10.1016/j.foodres.2013.03.008.

Saeed, R.M., Paul Schlegel, J., Castano Giraldo, C. H., Schlegel, J.P., Castano, C., & Sawafta, R. (2016). Uncertainty of thermal characterization of phase change material by differential scanning calorimetry analysis. https://www.researchgate.net/publication/291973182.

Schindler, S., Wittig, M., Zelena, K., Krings, U., Bez, J., Eisner, P., Berger, R.G., 2011. Lactic fermentation to improve the aroma of protein extracts of sweet lupin (Lupinus angustifolius). Food Chem. 128 (2), 330–337. https://doi.org/10.1016/j.foodchem.2011.03.024.

Schlegel, K., Leidigkeit, A., Eisner, P., Schweiggert-Weisz, U., 2019. Technofunctional and sensory properties of fermented lupin protein isolates. Foods 8 (12). https://doi.org/10.3390/foods8120678.

Schutyser, M.A.I., Pelgrom, P.J.M., van der Goot, A.J., Boom, R.M., 2015. Dry fractionation for sustainable production of functional legume protein concentrates. Trends Food Sci. Technol. 45 (2), 327–335. https://doi.org/10.1016/j.tifs.2015.04.013.

Shrestha, S., Hag, L.V.T., Haritos, V.S., Dhital, S, 2021. Lupin proteins: structure, isolation and application. In: Trends in Food Science and Technology, 116. Elsevier Ltd, pp. 928–939. https://doi.org/10.1016/j.tifs.2021.08.035. Vol.Issue.

Siccama, J.W., Pegiou, E., Zhang, L., Mumm, R., Hall, R.D., Boom, R.M., Schutyser, M.A.I., 2021. Maltodextrin improves physical properties and volatile compound retention of spray-dried asparagus concentrate. LWT 142 (2), 111058. https://doi.org/10.1016/j.lwt.2021.111058.

Sridharan, S., Meinders, M.B.J., Bitter, J.H., Nikiforidis, C.V., 2020. Pea flour as stabilizer of oil-in-water emulsions: protein purification unnecessary. Food Hydrocoll. 101 https://doi.org/10.1016/j.foodhyd.2019.105533.

Sweers, L.J.H., Mishyna, M., Boom, R.M., Fogliano, V., Keppler, J.K., Lakemond, C.M.M., 2023. Microfiltration for effective microbiological decontamination of edible insects – protein hydrolysis, aggregation and pH are critical for protein recovery. Food Bioprod. Process. 141, 128–138. https://doi.org/10.1016/j.fbp.2023.08.002.

Tabtabaei, S., Konakbayeva, D., Rajabzadeh, A.R., Legge, R.L., 2019. Functional properties of navy bean (Phaseolus vulgaris) protein concentrates obtained by pneumatic tribo-electrostatic separation. Food Chem. 283, 101–110. https://doi.org/10.1016/j.foodchem.2019.01.031.

Tang, C.H., Wang, X.Y., Yang, X.Q., Li, L., 2009. Formation of soluble aggregates from insoluble commercial soy protein isolate by means of ultrasonic treatment and their gelling properties. J. Food Eng. 92 (4), 432–437. https://doi.org/10.1016/j.jfoodeng.2008.12.017.

Torres, J.A., Chen, Y.C., Rodrigo-García, J., Jaczynski, J., 2007. Recovery of by-products from seafood processing streams. F. Shahidi Maximising the Value of Marine By-Products. Woodhead Publishing Series in Food Science, Technology and Nutrition, pp. 65–90. https://doi.org/10.1533/9781845692087.1.65.

Vitelli, M., Rajabzadeh, A.R., Tabtabaei, S., Assatory, A., Shahnam, E., Legge, R.L., 2020. Effect of hammer and pin milling on triboelectrostatic separation of legume flour. Powder Technol. 372 (7), 317–324. https://doi.org/10.1016/j.powtec.2020.06.007.

Wockenfuss, L., Lammers, V., Heinz, V., Sozer, N., Silventoinen-Veijalainen, P., 2023. Two steps of dry fractionation: comparison and combination of air classification and electrostatic separation for protein enrichment from defatted rapeseed press cake. J. Food Eng., 111623 https://doi.org/10.1016/j.jfoodeng.2023.111623.

Xing, Q., de Wit, M., Kyriakopoulou, K., Boom, R.M., Schutyser, M.A.I., 2018. Protein enrichment of defatted soybean flour by fine milling and electrostatic separation. Innov. Food Sci. Emerg. Technol. 50, 42–49. https://doi.org/10.1016/j.ifset.2018.08.014. December.

Xing, Q., de Wit, M., Kyriakopoulou, K., Boom, R.M., Schutyser, M.A.I., 2021. Effect of tube wall material on electrostatic separation of plant raw-materials. J. Food Process Eng. 44 (1), 1–9. https://doi.org/10.1111/jfpe.13575.

Yang, J., Kornet, R., Diedericks, C.F., Yang, Q., Berton-Carabin, C.C., Nikiforidis, C.V., Venema, P., van der Linden, E., Sagis, L.M.C., 2022. Rethinking plant protein extraction: albumin—from side stream to an excellent foaming ingredient. Food Struct. 31 https://doi.org/10.1016/j.foostr.2022.100254.

Yue, J., Gu, Z., Zhu, Z., Yi, J., Ohm, J.B., Chen, B., Rao, J., 2021. Impact of defatting treatment and oat varieties on structural, functional properties, and aromatic profile of oat protein. Food Hydrocoll. 112 https://doi.org/10.1016/j.foodhyd.2020.106368.

Zhang, Z., Wang, X., Yu, J., Chen, S., Ge, H., Jiang, L., 2017. Freeze-thaw stability of oil-in-water emulsions stabilized by soy protein isolate-dextran conjugates. LWT 78, 241–249. https://doi.org/10.1016/j.lwt.2016.12.051.

Zhong, Z.K., Sun, X.S., 2000. Thermal behavior and nonfreezing water of soybean protein components. Cereal Chem. 77 (4), 495–500. https://doi.org/10.1094/CCHEM.2000.77.4.495.

Zhou, X., Sala, G., Sagis, L.M.C., 2020. Bulk and interfacial properties of milk fat emulsions stabilized by whey protein isolate and whey protein aggregates. Food Hydrocoll. 109 https://doi.org/10.1016/j.foodhyd.2020.106100.